

# Millisecond kinetics of nanocrystal cation exchange using microfluidic X-ray absorption spectroscopy

*Emory M. Chan,<sup>‡</sup> Matthew A. Marcus,<sup>§</sup> Sirine Fakra,<sup>§</sup> Mariam S. Elnaggar,<sup>†</sup>*

*Richard A. Mathies,<sup>†</sup> A. Paul Alivisatos<sup>\*‡</sup>*

Department of Chemistry, University of California, Berkeley,

Materials Science Division, Lawrence Berkeley National Laboratory,

and Advanced Light Source, Lawrence Berkeley National Laboratory, Berkeley, CA 94720

\* To whom correspondence should be addressed. Email: [alivis@berkeley.edu](mailto:alivis@berkeley.edu)

<sup>†</sup> Dept. of Chemistry, UC-Berkeley

<sup>‡</sup> Materials Science Division, Lawrence Berkeley National Laboratory

<sup>§</sup> Advanced Light Source, Lawrence Berkeley National Laboratory

## Abstract

We describe the use of a flow-focusing microfluidic reactor to measure the kinetics of the CdSe-to-Ag<sub>2</sub>Se nanocrystal cation exchange reaction using micro-X-ray absorption spectroscopy ( $\mu$ XAS). The small microreactor dimensions facilitate the millisecond mixing of CdSe nanocrystal and Ag<sup>+</sup> reactant solutions, and the transposition of the reaction time onto spatial coordinates enables the *in situ* observation of the millisecond reaction with  $\mu$ XAS. XAS spectra show the progression of CdSe nanocrystals to Ag<sub>2</sub>Se over the course of 100 ms without the presence of long-lived intermediates. These results, along with supporting stopped flow absorption experiments, suggest that this nanocrystal cation exchange reaction is highly efficient and provide insight into how the reaction progresses in individual particles. This experiment illustrates the value and potential of *in situ* microfluidic X-ray synchrotron techniques for detailed studies of the millisecond structural transformations of nanoparticles and other solution-phase reactions in which diffusive mixing initiates changes in local bond structures or oxidation states.

KEYWORDS: microreactor, nanoparticle, *in situ*, XAS

## Introduction

Exchange reactions involving molecules in solution are kinetically limited by the collision rates and coordination of reagents, while exchange reactions in bulk solids are typically slower because they are limited by the diffusion of the exchanging species into the materials. Recently, nanoscale colloids in solution have been shown to participate in a variety of molecular-like reactions,<sup>1</sup> such as isomerization,<sup>2</sup> addition,<sup>3</sup> and exchange,<sup>4</sup> over much faster time scales than their bulk analogs. Nanocrystals offer a convenient medium to study the internal transformations of solids between the bulk and molecular scales if methods to probe such reactions *in situ* can be developed.

In one such nanocrystal exchange reaction, Son *et al.*<sup>4</sup> observed that silver(I) cations in solution can rapidly and reversibly replace the cadmium(II) cations in cadmium selenide nanocrystals, resulting in silver(I) selenide nanocrystals. Despite this wholesale cation exchange and rearrangement of the crystal lattice, the particles retain their nanoscale dimensions, and this transformation proceeds rapidly ( $\ll 1$  s) at room temperature in the nanocrystals<sup>4</sup> while proceeding slowly ( $>1$  hr) in bulk crystals.<sup>5</sup>

Explaining the fast kinetics of nanoscale cation exchange requires knowledge of the internal structure and composition of the nanocrystals as they react. While stopped-flow optical absorption could be used to obtain the general kinetics of this reaction, X-ray techniques such as X-ray Absorption Spectroscopy (XAS) offer direct insight into the oxidation states, coordination,<sup>6</sup> local order,<sup>7</sup> and surface properties<sup>8</sup> of reacting nanoparticles, even in the absence of a crystalline lattice.<sup>9</sup>

Unfortunately, traditional XAS techniques are limited to acquisition times of  $\sim 1$  to 1000 s per spectrum and require the averaging of numerous spectra for high quality data analysis.<sup>9</sup> A

handful of energy-dispersive EXAFS (ED-EXAFS) systems with stopped-flow instrumentation have demonstrated resolutions as low as 5 ms,<sup>10</sup> but they require the use of transmission detection and sample concentrations (>0.1 M) that are substantially larger than the typical  $\mu\text{M}$ -mM concentrations used for the CdSe $\rightarrow$ Ag<sub>2</sub>Se cation exchange reaction. Although XAS and small-angle X-ray scattering (SAXS) have been used to characterize the growth<sup>6,11</sup> and cation exchange<sup>7</sup> of concentrated nanocrystals on the time scale of minutes, the time and signal constraints of XAS at low concentration have prevented the *in situ* structural characterization of the millisecond cation exchange of CdSe nanoparticles.

Microfluidic devices can facilitate measurement of the time-dependent behavior of millisecond reactions through the devices' precise control, rapid mixing, and ability to transpose the reaction time onto spatial coordinates.<sup>12</sup> For fast reactions involving multiple reactant solutions, rapid mixing is essential for distinguishing diffusion effects from reaction kinetics. Due to the small diffusion lengths of microfluidic devices, millisecond mixing is possible and has been demonstrated in T-junctions,<sup>13</sup> hydrodynamically-focused jet mixers,<sup>14</sup> and in flowing plugs.<sup>15</sup> Since reaction time is proportional to the distance traveled, the time resolution is independent from the acquisition time, which is significant when detecting small signals as with X-ray scattering or absorption from dilute solutions. The utility of microfluidic devices for *in situ* X-ray characterization<sup>16-18</sup> has been demonstrated previously in applications such as using SAXS to probe the millisecond unfolding of proteins in a hydrodynamically focused microjet.<sup>19</sup> Similar microfluidic X-ray techniques should be useful for monitoring rapid nanoparticle reactions in microfluidic devices.<sup>20,21</sup>

To demonstrate the potential of microfluidic X-ray techniques for monitoring structural evolution in rapid nanoscale reactions, we describe the use of a microfluidic device to mix

reagents in a steady state, continuous flow scheme that enables the  $\text{CdSe} \rightarrow \text{Ag}_2\text{Se}$  nanocrystal cation exchange reaction to be probed *in situ* using XAS with millisecond resolution. A solution of cadmium selenide nanocrystals is mixed with a solution of silver(I) ions using a hydrodynamic focusing scheme based on that of Knight *et al.*<sup>14</sup> The smaller silver ions rapidly diffuse from the outer edges of a microchannel into a central nanocrystal stream to initiate the reaction, while the larger nanocrystals remain in the center of the microchannel due to laminar flow. The reaction is probed through a thin, X-ray-transparent silicon nitride window over the reaction channel using micro-XAS ( $\mu\text{XAS}$ ) acquired at the Se K-edge (12.66 keV). By acquiring spectra at different points along the channel, we are able to observe the cation exchange kinetics *in situ* down to 4 ms resolution. At mM CdSe concentrations, we observe the reaction to occur on the time scale of 100 ms, and we do not detect the presence of any intermediates that have significantly different spectra than the CdSe reactant or  $\text{Ag}_2\text{Se}$  product. We discuss this time scale in the context of collision efficiency and suggest how the cation exchange could progress inside individual crystals and across the total ensemble. Although signal limitations in this particular study prevented the collection of more revealing X-ray absorption fine structure, this study illustrates the feasibility of *in situ* microfluidic X-ray synchrotron techniques for studying the millisecond structural transformations of nanoscale materials and other species that undergo exchange reactions.

## Experimental

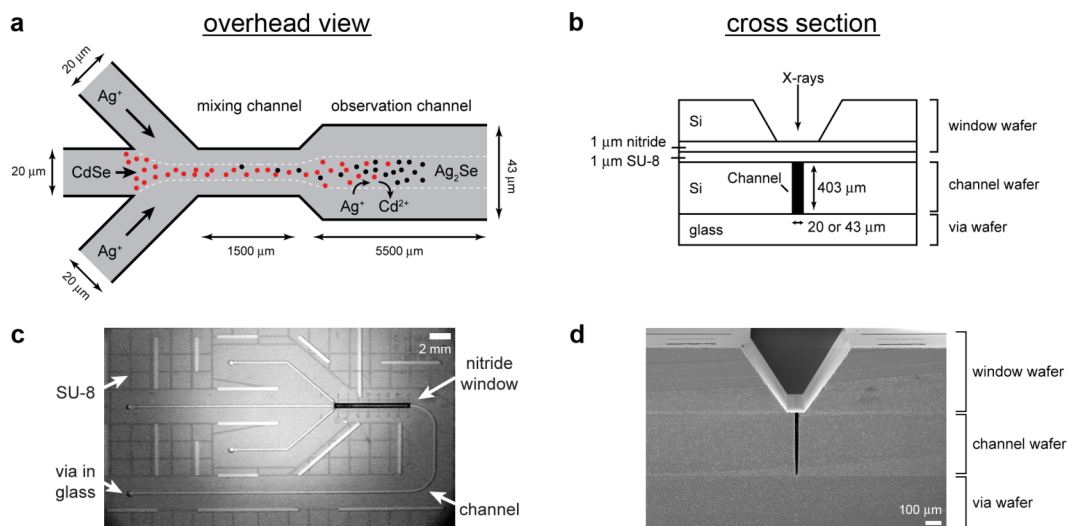


**Figure 1.** (a) Channel schematic of the XAS microreactor chip.  $\text{Ag}^+$  ions diffuse into the focused stream of CdSe nanocrystals and react to form  $\text{Ag}_2\text{Se}$  nanocrystals. Chip cross section (b) and overhead infrared image (c) showing the nitride membrane on the top window wafer, the SU-8 adhesion layer, the middle channel layer, and the bottom glass via layer. (d) SEM cross-section of the mixing channel.

**Device Design.** A schematic of the 110 nL, silicon-based microreactor is shown in Figure 1a. CdSe nanocrystal solution is injected via syringe pump into the center inlet, while  $\text{Ag}^+$  solution is injected into the two side inlets. After the three,  $20\ \mu\text{m}$ -wide inlet channels intersect, the nanocrystal stream is hydrodynamically focused as it enters the  $20\ \mu\text{m}$ -wide, 1.5 mm-long “mixing channel,” where the  $\text{Ag}^+$  ions diffuse rapidly into the  $\sim 7\ \mu\text{m}$ -wide CdSe stream. After mixing, the channel widens into a  $43\ \mu\text{m}$ -wide by  $403\text{-}\mu\text{m}$  deep by 5.5 mm-long “observation channel” so that the  $14\ \mu\text{m}$ -wide center nanocrystal stream can be more readily probed with a  $16 \times 7\ \mu\text{m}$  (horizontal  $\times$  vertical) X-ray spot through the  $100\ \mu\text{m}$ -wide nitride window aligned over

the channel. With typical flow rates of 12  $\mu\text{l}/\text{min}$  at each inlet (36  $\mu\text{l}/\text{min}$  total), the velocity in the center of the observation channel is  $1.5v_{avg} = 52 \mu\text{m}/\text{ms}$ , where  $v_{avg}$  is the average linear velocity.<sup>22</sup>

**Fabrication.** The microfluidic XAS device, whose cross-section is shown in Figure 1b, is fabricated as three separate layers: (1) a top, silicon “window” wafer, (2) a middle, silicon “channel” wafer, and (3) a bottom, glass “via” wafer. Detailed fabrication protocols are provided in the Supporting Information.

The window wafer is fabricated with 1  $\mu\text{m}$ -thick silicon nitride windows that allow the sample to be probed with  $\mu\text{XAS}$  with negligible window absorption (Figure S1a). The channel wafer contains high aspect ratio channels (43 x 403  $\mu\text{m}$  width x height) for flowing the reaction solutions. These channels are designed to be very narrow to facilitate rapid diffusion and to be very tall to maximize X-ray absorption. The high aspect ratio (>9:1 height:width) results in a uniform fluid velocity profile over 75% of the channel’s vertical axis, reducing the residence time distribution and improving time resolution. The bottom via wafer, fabricated from 575  $\mu\text{m}$ -thick borofloat glass to prevent diffraction of the incident X-rays, contains drilled holes for fluidic access to the channel layer.

The fluidic channels are enclosed by sealing the channel wafer between the window wafer and via wafer (Figure S1c). The glass via wafer is anodically bonded to the bottom of the Si channel wafer, while the nitride window wafer is bonded to the top of the channel wafer using 1  $\mu\text{m}$ -thick SU-8 photoresist (Microchem). Infrared images (Figure 1c) of the final devices show the SU-8 bonding to be relatively void-free, and scanning electron micrographs of chip cross-

sections (Figure 1d) clearly depict the tight seal generated by the bonding between the three layers.

To prevent nanoparticle deposition on channel walls during the reaction, the oxide-coated walls are silanized with 1H,1H,2H,2H-perfluorodecyltrichlorosilane (FDTS) from solution.<sup>21</sup> The robust FDTS/oxide passivation, coupled with the use of dodecylamine surfactant, prevented deposition of solids onto the walls and enabled individual devices to be run nearly continuously for >44 hours.

**Reagents and solutions.** All CdSe and Ag<sup>+</sup> solutions are prepared with a 5% wt/wt (232 mM) solution of dodecylamine (DDA) in toluene in order to solubilize the Ag<sub>2</sub>Se nanocrystals. Immediately prior to their use, solutions are filtered with 0.45 μm PTFE syringe filters and sparged with helium to prevent bubble formation in the channel.

CdSe nanocrystal solutions are prepared by dissolving tri-*n*-octylphosphine oxide-capped CdSe nanocrystals<sup>23</sup> (diameter = 3.6 ± 0.4 nm) in the DDA solution at a typical Cd<sup>2+</sup> concentration of 1.4 mM. “CdSe” concentrations always refer to the concentration of individual Cd<sup>2+</sup> or Se<sup>2-</sup> ions, and unless specified, reagent concentrations refer to the values before mixing.

Ag<sup>+</sup> solutions are prepared by dissolving anhydrous AgClO<sub>4</sub> in DDA stock solution for a typical Ag<sup>+</sup> concentration of 5 mM. [*Safety note: silver perchlorate is a potentially explosive compound, especially when dissolved in organic solvents and subsequently dried. The solutions used in this experiment were always dilute and used in small volumes.*]



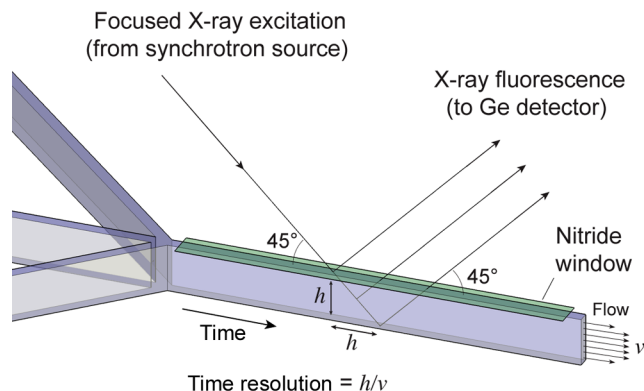


**Figure 2.** X-ray beam paths through the microreactor channel. Monochromated X-rays are focused through the window wafer’s nitride membrane and into the observation channel of the channel wafer at a 45° angle to the direction of flow. X-ray fluorescence is monitored at a 90° angle to the incident radiation. Due to the 45° angle of incidence, a channel with height  $h$  and linear particle velocity  $v$  has a time resolution of  $h/v$ .

**X-ray absorption spectroscopy.** X-ray synchrotron experiments were performed at Beamline 10.3.2 at the Advanced Light Source (ALS).<sup>24</sup> The microreactor chip is mounted in a custom-machined aluminum manifold on an x-y translation stage that allows time-resolved spectra to be recorded at various points along the channel. X-ray fluorescence elemental mapping is used to determine the location of the probe with respect to the reagent streams. As shown in Figure 2, a monochromated  $16 \times 7 \mu\text{m}$  (horizontal  $\times$  vertical) X-ray spot is focused through the nitride membrane onto the center of the CdSe stream at a 45° angle to the direction of fluid flow. X-ray fluorescence at the Se K-edge is collected with a 7-element germanium detector at a 90° angle with respect to the incident beam. The fluorescence signal is measured rather than the X-ray transmission because the emission intensity has better signal-to-noise ratio and is in principle linear with absorption at the short path lengths and dilute concentrations used in this experiment.  $\mu\text{XAS}$  spectra are collected by scanning the incident energy from 12.50 to 12.86 keV and recording the Se K-edge fluorescence integrated between 10.93 and 11.33 keV. Spectra of CdSe

and Ag<sub>2</sub>Se standard solutions were recorded in 1.5 mm-diameter borosilicate glass capillaries with 10 μm-thick walls.

Data points at each energy of a spectrum are normalized to the incident flux, and all spectra are background subtracted and normalized according to their average post-edge intensities. Four normalized sample spectra are averaged for each kinetic time point. The relative fractions of reactants and products for each time point are determined by fitting the averaged spectrum as a linear combination of the CdSe and Ag<sub>2</sub>Se standard spectra using least-squares regression routines in Igor Pro software.

The reaction time corresponding to each spectrum is  $t_{rxn} = t_{mix} + \Delta y_{obs}/v_{center}$ , where  $t_{mix}$  is the residence time for fluid flowing in the center of the mixing channel,  $\Delta y_{obs}$  is the distance of the X-ray spot from the entrance of the observation channel, and  $v_{center}$  is the linear flow velocity in the center of the observation channel. Because the incident X-ray radiation passes through the channel at a 45° angle with respect to the flow axis, the length of channel excited by the incident beam is equal to  $h$ , the channel height (Figure 2). The time resolution is therefore  $h/v_{center}$ , or 8 ms at  $v_{center} = 52 \mu\text{m/ms}$  (36 μL/min). We can also record spectra at  $v_{center} = 104 \mu\text{m/ms}$ , which improves the resolution to 4 ms, but high flow rates prevent the acquisition of data at longer residence times due to the finite length of the 5.5 mm-long observation channel.

**Stopped-flow absorption experiments.** Time-resolved optical absorption measurements are recorded in an Applied Photophysics stopped flow apparatus. CdSe and AgClO<sub>4</sub> solutions are injected in a 1:1 volumetric ratio through a 10 mm-path length cell. Absorption is measured at 600 nm ( $A_{600}$ ), which is slightly below the absorption edge of 3.6 nm CdSe nanocrystals but

above that of the low-band gap  $\text{Ag}_2\text{Se}$ . Since  $A_{600} = 0$  for CdSe nanocrystals, the percent conversion at time  $t$  is defined as  $A_{600}(t)/A_{600}(t \rightarrow \infty)$ .

## Results & Discussion

**Time-resolved  $\mu$ XAS.** Time-resolved Se K-edge XAS spectra (Figure 3) of 3.6 nm-diameter CdSe nanocrystals reacted with  $\text{Ag}^+$  ions in a flow-focusing microfluidic device clearly show the cation exchange of the particles from CdSe to  $\text{Ag}_2\text{Se}$  over the course of 100 ms. As evident in the disappearance of the CdSe peak at 12.673 keV, the Se K-edge spectra evolve from initially resembling the CdSe nanocrystal reference spectrum to resembling the  $\text{Ag}_2\text{Se}$  nanocrystal reference after 100 ms.

To quantify the progress of the cation exchange reaction over time, we fit each spectrum as a linear combination of the normalized CdSe and  $\text{Ag}_2\text{Se}$  standards, with the fraction of  $\text{Ag}_2\text{Se}$  ( $f_{\text{Ag}_2\text{Se}}$ ) indicating the progress of the reaction. As shown in Figure 3, the linear combinations fit the aforementioned  $\mu$ XAS spectra within the noise of the spectra and with no systematic residual. The excellent fits suggest that, within the temporal resolution (8 ms) and precision ( $f_{\text{Ag}_2\text{Se}} \pm 5\%$ ) of our procedure, there is no evidence for any significant population of intermediates that have appreciably different spectra from the standards. Principal component analysis<sup>25</sup> confirms that the set of spectra in Figure 3 can be described sufficiently as the weighted sums of just two independent components. The contributions of third primary component considered for completeness only improved the root mean square (rms) error in the linear fits from 1% to 0.7% and did not exhibit any coherent trend over time.

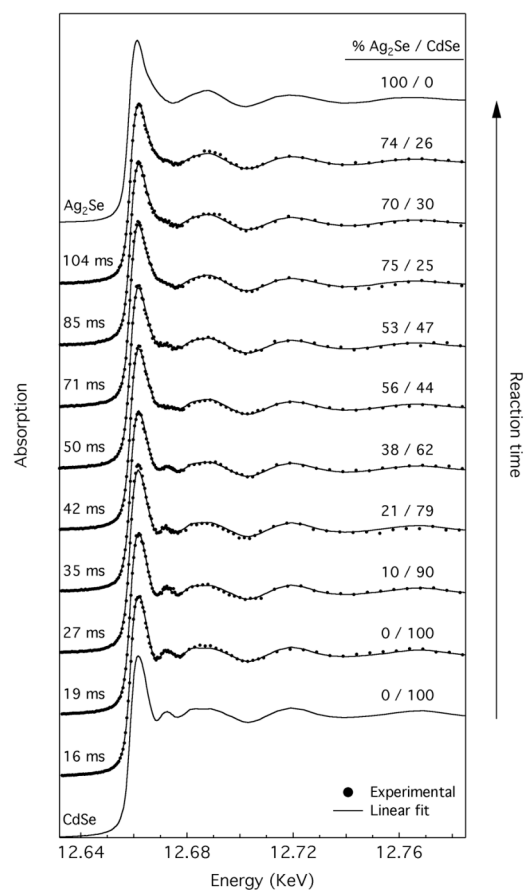


**Figure 3.** Time-resolved Se K-edge XAS spectra acquired *in situ* during the CdSe→Ag<sub>2</sub>Se nanocrystal cation exchange reaction using 1.4 mM CdSe and 5 mM AgClO<sub>4</sub> solutions in 5% wt dodecylamine in toluene. Each reaction time corresponds to a different position along the reactor channel. Ag<sub>2</sub>Se and CdSe compositions were extracted from fits performed using linear combinations of the Ag<sub>2</sub>Se and CdSe reference spectra (top and bottom).

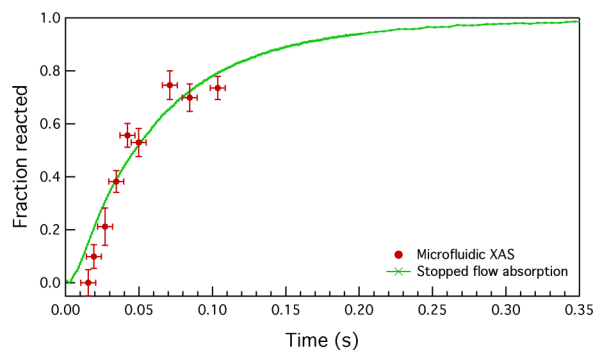


**Figure 4.** Fractional conversion vs. time using fit parameters extracted from XAS fits (1.4 mM CdSe, 5 mM AgClO<sub>4</sub>, red dots) and stopped flow experiments (1.4 mM CdSe, 6.67 mM AgClO<sub>4</sub> at 1:1 volumetric ratio, green line). Error bars show 95% confidence limits.

**Kinetic time traces:  $\mu$ XAS and stopped flow.** Kinetic curves ( $f_{Ag_2Se}$  vs. time, Figure 4) generated with the fit parameters extracted from the spectra in Figure 3 (1.4 mM CdSe/5 mM  $AgClO_4$ ) rise smoothly and monotonically until they flatten as reactants are depleted. Due to the finite length of the observation channel, the longest residence time that can be observed with microfluidic XAS at a flow rate of 36  $\mu$ l/min (52  $\mu$ m/ms) is 104 ms. Within this time regime, the  $\mu$ XAS-generated curve agrees well with the kinetic curve acquired using stopped-flow absorption at 600 nm, verifying the temporal accuracy of our microfluidic XAS technique.

The slight discrepancy between the microfluidic and stopped flow curves at short reaction times is likely due to the fact that the turbulent mixing during stopped flow is isolated to the first  $\sim$ 2 ms of the reaction, while the diffusion of the  $Ag^+$  ions into the center CdSe stream of the microfluidic device occurs continuously as they are simultaneously consumed by the reaction. Thus, at short reaction times in the microchannel, few  $Ag^+$  ions have had time to mix completely and react with the CdSe nanocrystals. The resulting low  $Ag_2Se$  fractions are difficult to resolve due to the noise in the XAS spectra (0.5% rms, relative to average intensity) compared to the modest difference ( $\sim$ 5% rms) between the remarkably similar  $Ag_2Se$  and CdSe Se K-edge reference spectra.

The stopped-flow trace in Figure 5 can be fit to the relevant integrated rate equation<sup>26</sup> for the bimolecular second-order rate equation,  $d[Ag_2Se]/dt = k[Ag^+][CdSe]$ , where the rate constant  $k = 6 \times 10^3 \text{ M}^{-1} \text{ s}^{-1}$ . While such a simple rate equation does not imply a specific mechanism, the good fit demonstrates that the general kinetic behavior of nanocrystal exchange reactions of small nanocrystals is similar to that of molecular exchange reactions.

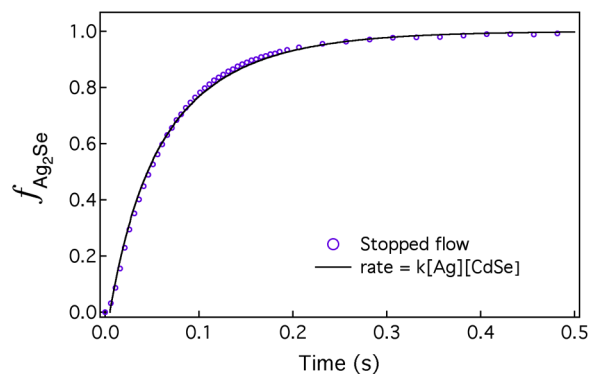


**Figure 5.** Comparison of the stopped flow kinetic curve (circles) with a 2<sup>nd</sup> order kinetics theoretical fit (line). Stopped flow was performed with 1.4 mM CdSe, 6.66 mM AgClO<sub>4</sub>. The 2<sup>nd</sup> order rate equation shown above was fit to the stopped flow data with a start time of 5 ms and  $k = 6 \times 10^3 \text{ M}^{-1} \text{ s}^{-1}$ .

**Interpretation via collision theory.** Both microfluidic XAS and stopped-flow absorption experiments were used to observe the cation exchange of CdSe nanocrystals in 3.33 mM Ag<sup>+</sup> and 5% wt DDA over a time scale of ~100 ms ( $1-1/e = 66$  ms). Since the time scale of this nanocrystal cation exchange reaction has not been measured previously, it is useful to discuss its physical context. We can use Smoluchowski diffusion theory<sup>27</sup> for bimolecular reactions to estimate<sup>28</sup> that at 3.33 mM Ag<sup>+</sup>,  $\sim 10^7$  Ag<sup>+</sup> ions will collide with each 3.6-nm nanocrystal over the 100 ms time scale of the cation exchange reaction, or  $\sim 10^4$  collisions are required to exchange one of the  $\sim 460$  Cd<sup>2+</sup> cations inside a 3.6 nm nanocrystal. Thus, on average, one out of every  $10^4$  Ag<sup>+</sup> collisions contributes to the cation exchange at room temperature. Such cation exchange efficiency is surprisingly high, given that the underlying process is a solid-state reaction that involves ions diffusing in a crystal lattice at room temperature. Assuming that every collision with kinetic energy greater than the activation barrier results in a cation exchange, the  $10^{-4}$  collision efficiency puts a ceiling on the activation energy at  $\sim 5$  kcal/mol, which is approximately the strength of a hydrogen bond. Such low activation energy and high collision

efficiency values, consistent with the fast reaction time, highlight the intrinsically different kinetics of the nanoscale reaction with respect to bulk and even molecular reactions.

**Surfactant effects.** While the small dimensions of the nanocrystals dramatically increase the kinetics of the cation exchange relative to bulk CdSe, the  $\sim 100$  ms time scale measured for nanocrystal cation exchange is much slower than the  $\sim 1$  ms estimated for the original CdSe $\rightarrow$ Ag<sub>2</sub>Se cation exchange experiments.<sup>29,30</sup> The cation exchange protocol detailed by Son *et al.*,<sup>4</sup> however, used silver(I) nitrate dissolved with methanol, whose enthalpically favorable solvation of Cd<sup>2+</sup> was hypothesized to be the driving force behind the rapid kinetics of cation exchange.<sup>4,31</sup> We observed, however, that the addition of methanol in 5 and 10% vol/vol amounts to the AgClO<sub>4</sub>/dodecylamine/toluene solutions only slightly increased the rate of exchange (Figure S3).

A more likely reason for the slower rate observed here is that the dodecylamine, necessary to keep the Ag<sub>2</sub>Se nanoparticles from aggregating on the microchannel walls, slows kinetics by reducing the availability of free Ag<sup>+</sup> ions and the accessibility of nanocrystal surfaces. Stopped flow experiments with 1.4 mM CdSe and 5 mM AgClO<sub>4</sub> at different concentrations of dodecylamine (DDA, Figure 6) show that the reaction is 90% complete after 3 ms at very low (1 mM) DDA concentrations, but slows down when the [DDA] is increased to 8 mM ( $f_{\text{Ag}_2\text{Se}} = 90\% @ 660$  ms). The further addition of DDA actually decreases the 90% conversion time to  $\sim 120$  ms. The fact that the kinetic effect of DDA reverses suddenly around DDA:Ag<sup>+</sup> = 4 (10 mM DDA, 2.5 mM Ag<sup>+</sup> after dilution) suggests that the dodecylamine hinders cation exchange primarily by forming tetrahedral complexes with Ag<sup>+</sup>. Increasing the [DDA]



beyond the saturation point of  $\text{Ag}^+$  increases the concentration of free DDA, which can solvate free  $\text{Cd}^{2+}$  ions and can increase the polarity of the solution.

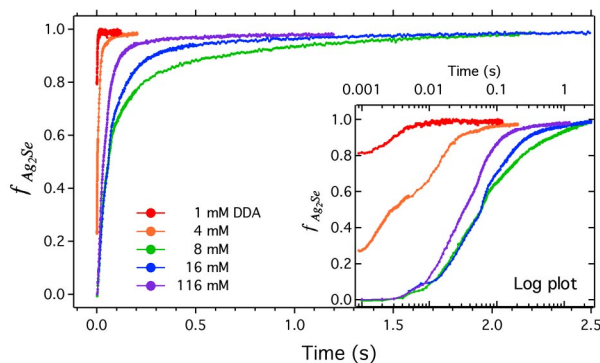


**Figure 6.** Stopped flow absorption curves at various dodecylamine (DDA) concentrations and 1.4 mM CdSe, 5 mM  $\text{AgClO}_4$ . Inset: log plot of the same data.

**Temporal distribution of cation exchange.** The structural and kinetic information from microfluidic XAS experiments provide insight into the behavior of the cation exchange reaction across the entire population of nanocrystals and within a single nanocrystal. Kinetic curves show that the total population of nanocrystals reacts over  $\sim 100$  ms, yet XAS spectra do not show any significant population of intermediates even at 8 ms resolution. The lack of observable intermediate Se states is surprising, because a partially reacted nanocrystal should contain at least one  $\text{Ag}_2\text{Se}/\text{CdSe}$  interface in which  $\text{Se}^{2-}$  ions are bound to some combination of  $\text{Cd}^{2+}$  ions,  $\text{Ag}^+$  ions, and vacancies. Given the sensitivity of the near-edge region of XAS spectra to the local geometry around the absorbing atoms, such interfacial  $\text{Se}^{2-}$  ions should exhibit distinct Se K-edge XAS spectra. A planar or shell-like monolayer of ions composes a significant fraction of the atoms in a 3.6 nm particle, which is only 10  $\text{Se}^{2-}$  ions in diameter. Therefore, if all nanocrystals

react in parallel, one would expect to observe statistically significant contributions from intermediate states in the XAS spectra.

The lack of spectral contributions from intermediates suggests the possibility that 3.6 nm nanocrystals may react in a distributed manner over the 100 ms required to react the entire ensemble of particles. Individual nanocrystals may react faster than the 8 ms resolution of our microfluidic XAS technique such that, on the time scale of our observation, all but an undetectable fraction of the nanocrystals are fully unreacted or fully reacted. The  $<8$  ms reaction times at low concentrations of dodecylamine (Figure 6) confirm that single particle conversion is not limited by solid-state diffusion or internal reaction kinetics on such short time scales. The short lifetimes of partially converted particles could also suggest that they are more reactive than unreacted CdSe particles, due to the high ionic mobility of  $\text{Ag}^+$  ions in  $\text{Ag}_2\text{Se}$ <sup>32</sup> or due to the less effective passivation of  $\text{Ag}_2\text{Se}$  surfaces by surfactants.

Clearly, more experiments and simulations need to be performed before a mechanism behind the nanoscale cation exchange reaction can be established. Stopped flow absorption experiments may be more practical for gathering single-wavelength kinetic data for determining rate orders and rate constants, but *in situ*  $\mu\text{XAS}$  is far more valuable for investigating the presence of intermediate states and the time-dependent nature of the nanocrystals' structural transformation. Due to time and signal constraints, the spectra collected for this experiment were too limited by signal and noise and were too narrow in energy range to perform rigorous EXAFS analysis. Our work does reveal means for improvement in collection efficiency, however, and at a beamline with improved flux, spectra should be clean enough to extract bond orders and geometries. The current time resolution is comparable to those of energy-dispersive EXAFS

(ED-EXAFS)<sup>9</sup>, but our technique is applicable to solutions too dilute to be detected in transmission mode, as ED-EXAFS requires. The decoupling of acquisition time and time resolution in microreactors should give future microfluidic XAS studies the advantages of traditional EXAFS at millisecond time-resolution.

## Conclusion

We have successfully fabricated a flow-focusing microreactor to observe the ~100 ms evolution of the CdSe→Ag<sub>2</sub>Se nanocrystal cation exchange reaction using micro X-ray absorption spectroscopy. The small dimensions of the reactor enable rapid mixing and *in situ* observation of the millisecond reaction with  $\mu$ XAS even with acquisition times of hundreds of seconds. XAS spectra clearly show the structural progression of CdSe nanocrystals to Ag<sub>2</sub>Se without the presence of long-lived intermediates, and kinetic curves can be generated by fitting the spectra with linear combinations of the reactant and product data. The time scale of the reaction, confirmed with stopped flow absorption experiments, is surprisingly slower than expected, most likely due to high concentrations of amines used to solubilize the product nanocrystals. The slower kinetics and the lack of observed intermediate states in the XAS spectra could suggest that the reaction consists of rapid single-particle reactions distributed over the 100 ms-time scale of the overall reaction. Detailed structural information about any intermediates should be possible with further refinements to the microfluidic XAS device to optimize signal and energy range, enabling the acquisition of full EXAFS spectra at various edges and even the collection of wide- and small-angle X-ray scattering data. The robust nature of this device also should allow the use of a wider range of chemicals and temperatures than all-polymer microdevices. With the ability to initiate reactions via diffusive mixing and the ability to

probe changes in local bond structure and oxidation state on the millisecond time scale, microfluidic XAS should be an indispensable tool for providing structural information in nanocrystal cation exchange reactions and other biological and chemical reactions where single-wavelength kinetics and traditional XAS methods are inadequate.

**Acknowledgements.** Chip fabrication was performed at the UC-Berkeley Microfabrication Laboratory. The authors thank Deborah Aruguete, Richard Robinson, and Donghee Son for helpful discussions, and Sanjay Krishnaswamy for assistance with stopped-flow measurements. This work was supported by the donors of the Center for Analytical Biotechnology and by the Director, Office of Energy Research, Office of Science, Division of Materials Sciences, of the U.S. Department of Energy under Contracts No. DE-AC03-76SF00098 and DE-AC02-05CH11231 (ALS).

**Supporting Information Available:** Chip fabrication schematic, powder X-ray diffraction patterns of reacted and unreacted nanocrystals, and kinetic curves for methanol tests. This material is available free of charge via the Internet at <http://pubs.acs.org>.

## References

- (1) Stellacci, F. *Nat. Mater.* **2005**, *4*, 113.
- (2) Jacobs, K.; Zaziski, D.; Scher, E. C.; Herhold, A. B.; Alivisatos, A. P. *Science* **2001**, *293*, 1803.
- (3) Yin, Y. D.; Rioux, R. M.; Erdonmez, C. K.; Hughes, S.; Somorjai, G. A.; Alivisatos, A. P. *Science* **2004**, *304*, 711.
- (4) Son, D. H.; Hughes, S. M.; Yin, Y. D.; Alivisatos, A. P. *Science* **2004**, *306*, 1009.
- (5) Leung, L. K.; Komplin, N. J.; Ellis, A. B.; Tabatabaie, N. *J. Phys. Chem.* **1991**, *95*, 5918.
- (6) Meneses, C. T.; Flores, W. H.; Sasaki, J. M. *Chem. Mater.* **2007**, *19*, 1024.
- (7) Wang, D. Y.; Chen, C. H.; Yen, H. C.; Lin, Y. L.; Huang, P. Y.; Hwang, B. J.; Chen, C. C. *J. Am. Chem. Soc.* **2007**, *129*, 1538.
- (8) Aruguete, D. M.; Marcus, M. A.; Li, L. s.; Williamson, A.; Fakra, S.; Gygi, F.; Galli, G. A.; Alivisatos, A. P. *J. Phys. Chem. C* **2007**, *111*, 75.
- (9) Newton, M. A.; Dent, A. J.; Evans, J. *Chem. Soc. Rev.* **2002**, *31*, 83.
- (10) Yoshida, N.; Matsushita, T.; Saigo, S.; Oyanagi, H.; Hashimoto, H.; Fujimoto, M. *J. Chem. Soc.-Chem. Commun.* **1990**, 354.
- (11) Meneau, F.; Sankar, G.; Morgante, N.; Winter, R.; Catlow, C. R. A.; Greaves, G. N.; Thomas, J. M. *Faraday Discuss.* **2003**, *122*, 203.
- (12) deMello, A. J. *Nature* **2006**, *442*, 394.
- (13) Kamholz, A. E.; Weigl, B. H.; Finlayson, B. A.; Yager, P. *Anal. Chem.* **1999**, *71*, 5340.

- (14) Knight, J. B.; Vishwanath, A.; Brody, J. P.; Austin, R. H. *Phys. Rev. Lett.* **1998**, *80*, 3863.
- (15) Song, H.; Tice, J. D.; Ismagilov, R. F. *Angew. Chem. Int. Ed.* **2003**, *42*, 768.
- (16) Akiyama, S.; Takahashi, S.; Kimura, T.; Ishimori, K.; Morishima, I.; Nishikawa, Y.; Fujisawa, T. *Proc. Natl. Acad. Sci. U. S. A.* **2002**, *99*, 1329.
- (17) Barrett, R.; Faucon, M.; Lopez, J.; Cristobal, G.; Destremaut, F.; Dodge, A.; Guillot, P.; Laval, P.; Masselon, C.; Salmon, J. B. *Lab Chip* **2006**, *6*, 494.
- (18) Greaves, E. D.; Manz, A. *Lab Chip* **2005**, *5*, 382.
- (19) Pollack, L.; Tate, M. W.; Finnefrock, A. C.; Kalidas, C.; Trotter, S.; Darnton, N. C.; Lurio, L.; Austin, R. H.; Batt, C. A.; Gruner, S. M.; Mochrie, S. G. *J. Phys. Rev. Lett.* **2001**, *86*, 4962.
- (20) Chan, E. M.; Mathies, R. A.; Alivisatos, A. P. *Nano Lett.* **2003**, *3*, 199.
- (21) Chan, E. M.; Alivisatos, A. P.; Mathies, R. A. *J. Am. Chem. Soc.* **2005**, *127*, 13854.
- (22)  $v_{center} = 1.5v_{avg}$  assuming two-dimensional laminar slot flow, which is valid at high channel aspect ratios.
- (23) Murray, C. B.; Norris, D. J.; Bawendi, M. G. *J. Am. Chem. Soc.* **1993**, *115*, 8706.
- (24) Marcus, M. A.; MacDowell, A. A.; Celestre, R.; Manceau, A.; Miller, T.; Padmore, H. A.; Sublett, R. E. *J. Synchrotron Rad.* **2004**, *11*, 239.
- (25) Manceau, A.; Marcus, M. A.; Tamura, N. Quantitative speciation of heavy metals in soils and sediments by synchrotron X-ray techniques. In *Applications of Synchrotron Radiation in Low-Temperature Geochemistry and Environmental Sciences*, 2002; Vol. 49; pp 341.

- (26) The overall 2nd order differential rate equation with 2:1 Ag<sup>+</sup>:CdSe stoichiometry can be integrated to derive the expression:

$$f_{Ag_2Se} = \left(1 - (M - 1) / \left(M \cdot \exp[2(M - 1)[CdSe]_o kt] - 1\right)\right),$$

where  $[CdSe]_o$  is the initial CdSe concentration,  $M = [Ag^+]_o/[CdSe]_o$ , and  $k$  is the 2<sup>nd</sup> order rate constant.

- (27) North, A. M. *The Collision Theory of Chemical Reactions in Liquids*; Wiley: New York, 1964; Vol. vii.
- (28) Collision frequency  $z = 4\pi(R_{Ag^+} + R_{CdSe})(D_{Ag^+} + D_{CdSe})[Ag^+]$ , where  $R$  is the radius and  $D$  is the Stokes-Einstein diffusion constant. Both species were assumed to be coordinated with dodecylamine. For a 3.6 nm-diameter nanocrystal with DDA,  $R_{CdSe}$  was calculated to be 3.4 nm.  $R_{Ag^+}$  was estimated to be a maximum of 1.7 nm.
- (29) The reaction time estimate was extracted from the size distribution of the reacted nanocrystals via Smoluchowski coagulation theory (Ref. 30). Our estimated 1 ms reaction time agrees with similar estimates by Son *et al.*
- (30) Smoluchowski, M. Z. *Phys. Chem.* **1917**, *92*, 129.
- (31) Burgess, J. *Metal Ions in Solution*; Wiley: New York, 1978.
- (32) Kobayashi, M. *Solid State Ionics* **1990**, *39*, 121.